Synchronous Controller between Drive Network of n Reaction-Diffusion Systems of FitzHugh - Nagumo type and Response Network of n Reaction-Diffusion Systems of Hindmarsh-Rose type

Phan Van Long Em

***Abstract*—This study explores the identical synchronization of drive-response neural networks consisting of n different reaction-diffusion systems with arbitrary structures. Specifically, the drive network is made up of n reaction-diffusion systems of FitzHugh-Nagumo type, while the response network contains n reaction-diffusion systems of Hindmarsh-Rose type. Despite the arbitrary topological structures of these two complex networks, we develop a nonlinear adaptive controller to achieve the desired synchronization. Additionally, the paper presents numerical results to validate the effectiveness of the proposed method.**

***Index Terms*—drive-response neural networks, identical synchronization, synchronous controller, reaction-diffusion system.**

I. Introduction

SYNCHRONIZATION is one of the most important dynamical properties of dynamical systems and has been extensively studied in various domains and natural phenomena, particularly in complex networks. There are various complex networks in nature and human society, including transportation networks, biological networks, social relationship networks, and neural networks, among others [5], [6], [8]. In recent years, complex networks have garnered significant interest in fields such as biology, engineering, economics, neuroscience, mathematics, and physics, and they have become a focal point of research in academic circles. Numerous valuable results have been obtained [1], [2], [3], [7], [15], [16]. Many studies delve into the synchronization of complex networks and its real-world applications [11], [12], [13], [14], [21]. The term "synchronization" typically refers to having the same behavior at the same time [5]. This principle is evident in various applications, including social production and human activities, such as ensuring communication security, developing laser equipment, and creating nuclear magnetic resonance instruments [12], [21].

The synchronization of complex networks has profound practical implications and has been extensively studied. Internal synchronization in complex networks has been explored in numerous papers, including references such as [1], [2]. Synchronization between two networks with distinct cell groups and structures is also achievable. This paper delves into the study of identical synchronization of drive-response neural networks with varying node dynamics. For example, in Fig. 1, the left graph illustrates the drive network, composed of n reaction-diffusion systems of FitzHugh-Nagumo type, while the right graph represents the response network with n reaction-diffusion systems of Hindmarsh-Rose type. Synchronizing networks with different structures and connections presents a formidable challenge, driving the investigation of a nonlinear controller design to realize identical synchronization of networks with differing node dynamics and topological structures.

In our research, we are exploring the concept of identical synchronization in neural networks. A neural network is a collection of neurons that are connected through physiological means, predominantly electrochemical processes [7]. This type of network is well-known in fields such as neurophysiology, automatic control, and image processing.

Our focus is on studying the synchronization of two or three reaction-diffusion systems of the FizHugh-Nagumo type [1], [2], as well as the synchronization of n dynamical systems of FitzHugh-Nagumo type in complete networks [18], [19], [20]. We have also conducted research on identical synchronization in a complete network of n reaction-diffusion systems of Hindmarsh-Rose type with both linear and nonlinear coupling [16], [15].

A significant gap in the existing literature is the lack of studies on the identical synchronization of two neural networks consisting of n distinct reaction-diffusion systems. This prompted us to select this topic, which specifically investigates the problem of identical synchronization for drive-response neural networks of n different reaction-diffusion systems. In this scenario, the drive network comprises n reaction-diffusion systems of FitzHugh-Nagumo type, while the response network contains n reaction-diffusion systems of Hindmarsh-Rose type.

Synchronizing two different systems is challenging, and synchronizing two networks with distinct dynamic nodes presents an even greater challenge. Our objective is to develop a controller that facilitates synchronization in such cases. In situations where the topological structures of the drive-response neural networks are known, we plan to design an appropriate nonlinear adaptive controller to achieve identical synchronization of these two networks. This will be based on Lyapunov stability theory and LaSalle's invariance

Manuscript received June 10, 2024; revised September 10, 2024.

This research is funded by Vietnam National University HoChiMinh City (VNU-HCM) under grant number C2024-16-03.

Phan Van Long Em is a lecturer of An Giang University, Vietnam National University, Ho Chi Minh City, VIETNAM (e-mail: pvlem@agu.edu.vn).

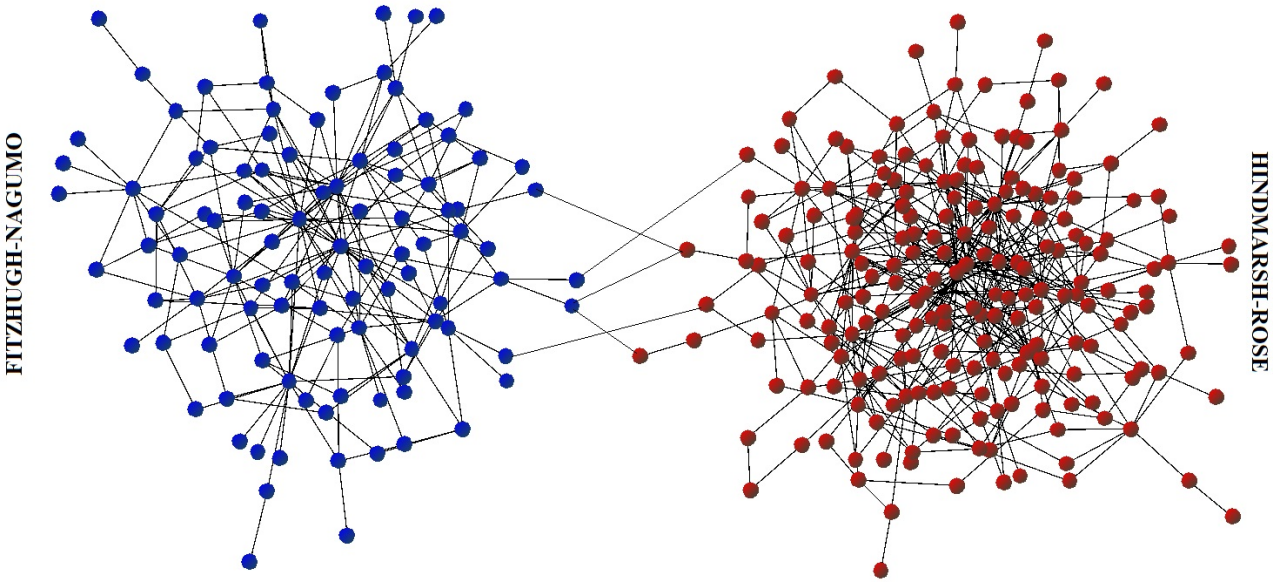

Fig. 1. This figure is an example of the drive-response networks of reaction-diffusion systems. On the left-hand side, there are n reaction-diffusion systems of FitzHugh-Nagumo type forming the drive network, and on the right-hand side, there are n reaction-diffusion systems of Hindmarsh-Rose type forming the response network.

principle. Additionally, we will present numerical results to validate the effectiveness of the proposed method.

This paper is structured as follows: In Section 2, we provide the definition of identical synchronization between the drive-response complex networks of n different reaction-diffusion systems and some preliminary knowledge. We also utilize the Lyapunov theory and LaSalle's invariance principle to design schemes for constructing the synchronous controller to achieve identical synchronization. In Section 3, we present two numerical examples to demonstrate the effectiveness of the method proposed in Section 2. Finally, in Section 4, we offer our conclusions.

II. Synchronous controller between drive network of n reaction-diffusion systems of FitzHugh - Nagumo type and response network of n reaction-diffusion systems of Hindmarsh-Rose type

In 1952, A. L. Hodgkin and A. F. Huxley revolutionized the field by introducing a groundbreaking four-dimensional mathematical system that accurately approximated neural membrane potential properties [7], [8], [10]. This led to the development of simpler models by numerous scientists to describe neuron voltage dynamics. Following suit, in 1962, R. FitzHugh and J. Nagumo unveiled the simplified two-dimensional FitzHugh-Nagumo model, derived from Hodgkin-Huxley's renowned model [11]. Despite its simplicity, this model yields incredible analytical results and preserves the energizing properties and biological significance of cells. The system comprises two equations in the variables u and v, where $u = u(t)$ represents the fast, excitatory transmembrane voltage and $v = v(t)$ represents the slow recovery variable, reflecting physical quantities like the electrical conductivity of ion currents across the membrane. The ordinary differential equations of the FitzHugh-Nagumo type are given by [1], [2]:

$$\begin{cases} \varepsilon \dfrac{du}{dt} = \varepsilon u_t = f(u) - v + I, \\ \dfrac{dv}{dt} = v_t = au - bv + c, \end{cases} \tag{1}$$

where a, b, c are constants (a, b are strictly positive); $0 < \varepsilon < 1$; $f(u) = -u^3 + 3u$; I presents the external current; t presents the time.

In 1982, J. L. Hindmarsh and R. M. Rose introduced a new, simpler model called the Hindmarsh-Rose model [9]. This model is as simple as the FitzHugh-Nagumo model, and consists of two equations in two variables, $\overline{u}$ and $\overline{v}$. The first variable represents the transmembrane voltage, and the second represents some physical quantities, such as the electrical conductivity of ion currents across the membrane. The ordinary differential equations of Hindmarsh-Rose type are given by [7].

$$\begin{cases} \dfrac{d\overline{u}}{dt} = \overline{u}_t = g(\overline{u}) + \overline{v} + \overline{I}, \\ \dfrac{d\overline{v}}{dt} = \overline{v}_t = 1 - \overline{b}u^2 - \overline{v}, \end{cases} \tag{2}$$

where $\overline{u} = \overline{u}(t), \overline{v} = \overline{v}(t)$; $g(\overline{u}) = -\overline{u}^3 + \overline{a}.\overline{u}^2$; the parameters $\overline{a}, \overline{b}$ are positive constants determined by practical experience; $\overline{I}$ presents the external current; t presents the time.

The systems (1) and (2) are insufficient in describing the propagation of action potential along the axon. To address this limitation, we have investigated the cable equation, which involves adding the Laplace operator of transmembrane voltage to the first equation of systems (1) and (2). This approach yields models that not only describe the propagation of action potential, but also provide insights into quantitative and qualitative cell functioning. Consequently, we are considering the reaction-diffusion system of

FitzHugh-Nagumo type (FHN) as follows:

$$\begin{cases} \varepsilon u_t = f(u) - v + I + d\Delta u, \\ \\ v_t = au - bv + c, \end{cases} \tag{3}$$

where $u = u(x,t),\ v = v(x,t),\ (x,t) \in \Omega \times \mathbb{R}^+;\ d$ is a positive constant; Δu is the Laplace operator of u; $\Omega \subset \mathbb{R}^N$ is a regular bounded open set and with Neumann zero flux boundary conditions, and N is a positive integer.

The reaction-diffusion system of Hindmarsh-Rose type (HR) is as follows:

$$\begin{cases} \overline{u}_t = g(\overline{u}) + \overline{v} + \overline{I} + \overline{d}\Delta\overline{u}, \\ \\ \overline{v}_t = 1 - \overline{b}u^2 - \overline{v}, \end{cases} \tag{4}$$

where $\overline{u} = \overline{u}(x,t),\ \overline{v} = \overline{v}(x,t),\ (x,t) \in \Omega \times \mathbb{R}^+;\ \overline{d}$ is a positive constant; $\Delta\overline{u}$ is the Laplace operator of $\overline{u}$; Ω and N are defined as in system (3).

These models offer a comprehensive representation of various physiological patterns and phenomena. They comprise two nonlinear partial differential equations, with the first equation capturing the action potential and the second one introducing the recovery variable to describe essential physical quantities. Notably, the first equation closely resembles the cable equation, portraying the distribution of membrane potential along the axon of a single cell [8], [11]. Additionally, systems (3) and (4) are effectively treated as a neural model, and networks of n coupled systems (3) and (4) are thoughtfully constructed as follows:

$$\begin{cases} \varepsilon u_{it} = f(u_i) - v_i + I_i + d_i\Delta u_i + \sum\limits_{j=1}^{n} c_{ij}h(u_i,u_j), \\ v_{it} = au_i - bv_i + c, \\ i = 1,2,...,n, \end{cases} \tag{5}$$

and

$$\begin{cases} \overline{u}_{it} = g(\overline{u}_i) + \overline{v}_i + \overline{I}_i + \overline{d}_i\Delta\overline{u}_i + \sum\limits_{j=1}^{n} \overline{c}_{ij}\overline{h}(\overline{u}_i,\overline{u}_j) + w_i, \\ \overline{v}_{it} = 1 - \overline{b}\overline{u}_i^2 - \overline{v}_i + \overline{w}_i, \\ i = 1,2,...,n, \end{cases} \tag{6}$$

where $(u_i,v_i),\ (\overline{u}_i,\overline{v}_i), I_i, \overline{I}_i, d_i, \overline{d}_i, i = 1,2,...,n$ are defined as (3) and (4), respectively. The coefficients c_{ij} are the elements of the connectivity matrix $C_n = (c_{ij})_{n\times n}$, defined by: $c_{ij} > 0$ if neuron ith and jth are coupled, $c_{ij} = 0$ if neuron ith and jth are not coupled. This matrix also presents the network topology. The function h presents the coupling function describing the type of connection between cell ith and jth. It is known that neurons connect through synapses, then it leads to two types of connections between cells such as chemical connections and electrical ones. The coefficients $\overline{c}_{ij}$ and the function $\overline{h}$ are defined as c_{ij} and h in system (5), respectively; $w_i, \overline{w}_i, i = 1,2,...,n$ are the synchronous controllers to be designed.

If the neurons are connected through a chemical synapse, then the coupling function is nonlinear [1], [2], [7] and is defined by the following formula:

$$h(u_i,u_j) = -(u_i - V_{syn})g_{syn}\frac{1}{1+\exp(-\lambda(u_j - \theta_{syn}))}, \tag{7}$$

for all $i,j = 1,2,...,n,\ j \neq i$, where g_{syn} represents a positive number that is called the coupling strength [6], [7], [8]; the variable V_{syn} represents the reversal potential, and it must have a value larger than $u_i(x,t)$, for all $i = 1,2,...,n$, $x \in \Omega, t \geq 0$ since synapses are considered to be excitatory; the symbol θ_{syn} indicates the threshold value that is reached by every action potential; λ is a positive number that can be large enough to approximate the Heaviside function [6], [7].

If neurons are connected through an electrical synapse, the coupling function is linear [7], [15]. It is given by the following formula:

$$h(u_i,u_j) = -g_{syn}(u_i - u_j), \tag{8}$$

for all $i,j = 1,2,...,n,\ j \neq i$.

The network represented by (5) is the drive network, while the network represented by (6) is the response network. From the model of drive-response neural networks, it is evident that the topologies of the two networks can differ, and the node dynamics are also distinct. Due to these differences, achieving identical synchronization of the two networks without adding any controllers is impossible. Therefore, designing adaptive controllers is necessary to achieve the desired synchronization.

Before we delve into the main results, it's crucial to consider the following remarks to substantiate our desired outcomes.

Remark 1. The function f satisfies the following condition:

$$|f(u_i) - f(u_j)| \leq \alpha_1 |u_i - u_j|,\ i,j = 1,2,...,n, \tag{9}$$

where u_i, u_j present the transmembrane voltages, and α_1 is a positive number.

Proof: For all $u_i, u_j, i, j = 1,2,...,n$, we have:

$$\begin{aligned} f(u_i) - f(u_j) &= -u_i^3 + 3u_i + u_j^3 - 3u_j \\ &= (u_i - u_j)\left[3 - (u_i - u_j)^2 - u_iu_j\right]. \end{aligned}$$

Since $u_i, u_j, i, j = 1,2,...,n$ are bounded in [3], then we can find a positive constant α_1 such that:

$$|f(u_i) - f(u_j)| \leq \alpha_1 |u_i - u_j|,\ i,j = 1,2,...,n.$$

■

Remark 2. The function g satisfies the following condition:

$$|g(\overline{u}_i) - g(\overline{u}_j)| \leq \alpha_2 |\overline{u}_i - \overline{u}_j|,\ i,j = 1,2,...,n, \tag{10}$$

where $\overline{u}_i, \overline{u}_j$ present the transmembrane voltages, and α_2 is a positive number.

Proof: For all $\overline{u}_i, \overline{u}_j, i, j = 1,2,...,n$, we have:

$$\begin{aligned} g(\overline{u}_i) - g(\overline{u}_j) &= -\overline{u}_i^3 + \overline{a}.\overline{u}_i^2 + \overline{u}_j^3 - \overline{a}.\overline{u}_j^2 \\ &= (\overline{u}_i - \overline{u}_j)\left[\overline{a}(\overline{u}_i + \overline{u}_j) - (\overline{u}_i^2 + \overline{u}_i.\overline{u}_j + \overline{u}_j^2)\right]. \end{aligned}$$

Since $\overline{u}_i, \overline{u}_j, i, j = 1,2,...,n$ are bounded in [17], then we can find a positive constant α_2 such that:

$$|g(\overline{u}_i) - g(\overline{u}_j)| \leq \alpha_2 |\overline{u}_i - \overline{u}_j|,\ i,j = 1,2,...,n.$$

■

Remark 3. The function h defined by (7) satisfies the following condition:

$$|h(u_i,u_k) - h(u_j,u_l)| \leq \beta |u_i - u_j|,\ i,j,k,l = 1,2,...,n, \tag{11}$$

where u_i, u_j, u_k, u_l present the transmembrane voltages, and β is a positive number.

Proof: For all $u_i, u_j, i, j = 1, 2, ..., n$, we have:

$$|h(u_i, u_k) - h(u_j, u_l)| = \\ = \left| g_{syn}(u_i - V_{syn}) \frac{1}{1 + \exp(-\lambda(u_k - \theta_{syn}))} \right. \\ \left. - g_{syn}(u_j - V_{syn}) \frac{1}{1 + \exp(-\lambda(u_l - \theta_{syn}))} \right|,$$

where $k \neq i, l \neq j$.

Since $u_k, u_l, k, l = 1, 2, ..., n$ are bounded in [3], then we can find a positive constant K such that:

$$-K \leq \frac{1}{1 + \exp(-\lambda(u_k - \theta_{syn}))} \leq K,$$

and

$$-K \leq \frac{1}{1 + \exp(-\lambda(u_l - \theta_{syn}))} \leq K.$$

Besides that $u_i - V_{syn} < 0$; $u_j - V_{syn} < 0$, for all $u_i, u_j, i, j = 1, 2, ..., n$, since we only consider the rapid chemical excitatory synapses [6], [7].

Thus,

$$|h(u_i, u_k) - h(u_j, u_l)| \leq \\ \leq |K g_{syn}(u_i - V_{syn}) + K g_{syn}(u_j - V_{syn})| \\ \leq K g_{syn} |u_i + u_j - 2V_{syn}|.$$

Moreover, $u_i, u_j, i, j = 1, 2, ..., n$ are bounded in [3], then we can find a positive constant β such that:

$$|h(u_i, u_k) - h(u_j, u_l)| \leq \beta |u_i - u_j|.$$

■

Remark 4. It is easy to see that the function h defined by (8) satisfies the following condition:

$$|h(u_i, u_k) - h(u_j, u_l)| \leq \beta |u_i - u_j|, \ i, j, k, l = 1, 2, ..., n, \tag{12}$$

where u_i, u_j, u_k, u_l present the transmembrane voltages, and β is a positive number.

Remark 5. The function $\overline{h}$ in network (6) is defined as h in network (5), then it also verifies the conditions in Remark 3 and Remark 4.

Remark 6. We can take the system (6) as the drive network and the system (5) as the response one. Then, all proofs in this work could be realized in the same manner.

We remind that the identical synchronization in the network of n reaction-diffusion systems is expressed as follows.

Definition 1 (see [1])**.** *Let $S_i = (u_i, v_i)$, $i = 1, 2, ..., n$ and $S = (S_1, S_2, ..., S_n)$ be a network. We say that S is identically synchronous if*

$$\lim_{t \to +\infty} \sum_{i=1}^{n-1} \left(\|u_i - u_{i+1}\|_{L^2(\Omega)} + \|v_i - v_{i+1}\|_{L^2(\Omega)} \right) = 0,$$

where $L^2(\Omega)$ is function space on Ω defined using a natural generalization of the 2-norm for finite-dimensional vector spaces.

By applying Definition 1 to this work, we let the node error of the identical synchronization between two systems (5) and (6) be $e_i = \overline{u}_i - u_i, \overline{e}_i = \overline{v}_i - v_i$, $i = 1, 2, ..., n$. If there is a controller w_i such that Definition 1 satisfies, it means:

$$\lim_{t \to +\infty} \sum_{i=1}^{n} \left(\|e_i\|_{L^2(\Omega)} + \|\overline{e}_i\|_{L^2(\Omega)} \right) = 0,$$

then the networks (5) and (6) are said to be identical synchronization.

To get the identical synchronization of networks (5) and (6), the controller w_i is designed as follows:

$$w_i = u_{it} - g(u_i) - v_i - \overline{I}_i - \overline{d}_i \Delta u_i - \sum_{j=1}^{n} \overline{c}_{ij} \overline{h}(u_i, u_j) - k_i e_i, \tag{13}$$

and

$$\overline{w}_i = v_{it} - 1 + \overline{b} u_i^2 + v_i - \overline{k}_i . \overline{e}_i, \tag{14}$$

with the updated rules defined as follows:

$$k_{it} = r_i e_i^2, \text{ and } \overline{k}_{it} = \overline{r}_i . \overline{e}_i^2, \tag{15}$$

where $r_i, \overline{r}_i$ are arbitrary positive constants, for $i = 1, 2, ..., n$.

Under the action of the controllers, the error dynamic equations of the system is described as follows:

$$\begin{aligned} e_{it} &= (\overline{u}_{it} - u_{it}) \\ &= g(\overline{u}_i) + \overline{v}_i + \overline{I}_i + \overline{d}_i \Delta \overline{u}_i + \sum_{j=1}^{n} \overline{c}_{ij} \overline{h}(\overline{u}_i, \overline{u}_j) \\ &\quad - g(u_i) - v_i - \overline{I}_i - \overline{d}_i \Delta u_i - \sum_{j=1}^{n} \overline{c}_{ij} \overline{h}(u_i, u_j) - k_i e_i \\ &= g(\overline{u}_i) - g(u_i) + (\overline{v}_i - v_i) + \overline{d}_i \Delta (\overline{u}_i - u_i) \\ &\quad + \sum_{j=1}^{n} \overline{c}_{ij} (\overline{h}(\overline{u}_i, \overline{u}_j) - \overline{h}(u_i, u_j)) - k_i e_i, \end{aligned} \tag{16}$$

and

$$\overline{e}_{it} = \overline{v}_{it} - v_{it} = -\overline{b}(\overline{u}_i^2 - u_i^2) - (\overline{v}_i - v_i) - \overline{k}_i . \overline{e}_i, \tag{17}$$

for $i = 1, 2, ..., n$.

Next, we explore the identical synchronization issue of networks (5) and (6). The primary result is presented in the following theorem.

Theorem 1. *The drive-response neural networks* (5) *and* (6) *can achieve identical synchronization under the adaptive controllers* (13)*,* (14) *and updated rules* (15)*.*

Proof: We construct the Lyapunov function as follows:

$$V(x, t) = \frac{1}{2} \sum_{i=1}^{n} \int_{\Omega} \left[e_i^2 + \overline{e}_i^2 + \frac{1}{r_i} (k_i - k)^2 + \frac{1}{\overline{r}_i} (\overline{k}_i - \overline{k})^2 \right] dx, \tag{18}$$

where $k, \overline{k}$ are positive constants to be determined.

Calculating the time derivative of $V(x, t)$, we get:

$$\frac{\partial V(x, t)}{\partial t} = \sum_{i=1}^{n} \int_{\Omega} \left[e_i e_{it} + \bar{e}_i \bar{e}_{it} + \frac{1}{r_i} (k_i - k) k_{it} \right. \\ \left. + \frac{1}{\bar{r}_i} (\bar{k}_i - \bar{k}) \bar{k}_{it} \right] dx. \tag{19}$$

By using the error systems (16) and (17), (19) becomes:

$$\frac{\partial V(x,t)}{\partial t} = \sum_{i=1}^{n} \int_{\Omega} [e_i \left(g(\overline{u}_i) - g(u_i) + (\overline{v}_i - v_i)\right.$$
$$+\overline{d}_i \Delta(\overline{u}_i - u_i) + \sum_{j=1}^{n} \overline{c}_{ij}(\overline{h}(\overline{u}_i, \overline{u}_j) - \overline{h}(u_i, u_j)) - k_i e_i)$$
$$+\overline{e}_i \left(\overline{b}(\overline{u}^2{}_i - u_i^2) - (\overline{v}_i - v_i) - \overline{k}_i.\overline{e}_i\right)$$
$$+\frac{1}{r_i}(k_i - k)k_{it} + \frac{1}{\overline{r}_i}(\overline{k}_i - \overline{k})\overline{k}_{it}]dx. \tag{20}$$

By using the Green formula and Neumann zero flux boundary conditions, (20) becomes:

$$\frac{\partial V(x,t)}{\partial t} \leq \sum_{i=1}^{n} \int_{\Omega} [e_i \left(g(\overline{u}_i) - g(u_i)\right) + e_i \overline{e}_i$$
$$+e_i \sum_{j=1}^{n} \overline{c}_{ij}(\overline{h}(\overline{u}_i, \overline{u}_j) - \overline{h}(u_i, u_j)) - k_i e_i^2 + \overline{b} e_i \overline{e}_i (\overline{u}_i + u_i)$$
$$-\overline{k}_i \overline{e}_i^2 - \overline{e}_i^2 + k_i e_i^2 - k e_i^2 + \overline{k}_i \overline{e}_i^2 - \overline{k} \overline{e}_i^2] \, dx$$
$$\leq \sum_{i=1}^{n} \int_{\Omega} [e_i \left(g(\overline{u}_i) - g(u_i)\right) + e_i \overline{e}_i$$
$$+e_i \sum_{j=1}^{n} \overline{c}_{ij}(\overline{h}(\overline{u}_i, \overline{u}_j) - \overline{h}(u_i, u_j)) + \overline{b} e_i \overline{e}_i (\overline{u}_i + u_i)$$
$$-(1 + \overline{k})\overline{e}_i^2 - k e_i^2] \, dx. \tag{21}$$

By using Remarks 1-6, it is easy to obtain:

$$\frac{\partial V(x,t)}{\partial t} \leq \sum_{i=1}^{n} \int_{\Omega} \left[\alpha_2 e_i^2 - (1 + \overline{k})\overline{e}_i^2 - k e_i^2 \right.$$
$$\left. + |e_i| \, |\overline{e}_i| \, (1 + \overline{b}(|\overline{u}_i| + |u_i|)) + \sum_{j=1}^{n} \beta \, |\overline{c}_{ij}| \, |e_i| \, |e_j| \right] dx. \tag{22}$$

Besides that, we can see:

$$\sum_{i=1}^{n}\sum_{j=1}^{n} \beta \, |\overline{c}_{ij}| \, |e_i| \, |e_j| = \beta \sum_{i=1}^{n} \left(|e_i| \sum_{j=1}^{n} |\overline{c}_{ij}| \, |e_j| \right)$$
$$\leq \beta \left(\sum_{i=1}^{n} e_i^2 . \sum_{i=1}^{n} \left(\sum_{j=1}^{n} |\overline{c}_{ij}| \, |e_j| \right)^2 \right)^{\frac{1}{2}}$$
$$\leq \beta \left(\sum_{i=1}^{n} e_i^2 . \sum_{i=1}^{n} \left(\sum_{j=1}^{n} \overline{c}_{ij}{}^2 . \sum_{j=1}^{n} e_j^2 \right) \right)^{\frac{1}{2}}$$
$$\leq \beta \left(\left(\sum_{i=1}^{n} e_i^2 \right)^2 . \sum_{i=1}^{n} \left(\sum_{j=1}^{n} \overline{c}_{ij}{}^2 \right) \right)^{\frac{1}{2}}$$
$$\leq \beta \left(\left(\sum_{i=1}^{n} e_i^2 \right)^2 . n^2 \max_{1 \leq i,j \leq n} \overline{c}_{ij}{}^2 \right)^{\frac{1}{2}}$$
$$\leq \beta n \max_{1 \leq i,j \leq n} |\overline{c}_{ij}| \sum_{i=1}^{n} e_i^2, \tag{23}$$

and

$$|e_i| \, |\overline{e}_i| \, (1 + \overline{b}(|\overline{u}_i| + |u_i|)) \leq \frac{1}{2}(1 + \overline{b}(|\overline{u}_i| + |u_i|))(e_i^2 + \overline{e}_i^2)$$
$$\leq M(e_i^2 + \overline{e}_i^2), \tag{24}$$

where M is a positive constant, since $u_i, \overline{u}_i, i = 1, 2, ..., n$ are bounded (see [3], [17]).

Combining (22), (23) and (24) yields:

$$\frac{\partial V(x,t)}{\partial t} \leq \sum_{i=1}^{n} \int_{\Omega} [\alpha_2 e_i^2 - (1 + \overline{k})\overline{e}_i^2 - k e_i^2$$
$$+M e_i^2 + M \overline{e}_i^2 + \beta n \max_{1 \leq i,j \leq n} |\overline{c}_{ij}| \, e_i^2] dx$$
$$\leq \sum_{i=1}^{n} \int_{\Omega} [(\alpha_2 - k + M + \beta n \max_{1 \leq i,j \leq n} |\overline{c}_{ij}|) e_i^2$$
$$-(1 + \overline{k} - M)\overline{e}_i^2] dx$$
$$\leq \sum_{i=1}^{n} \int_{\Omega} [-(k - \alpha_2 - M - \beta n \max_{1 \leq i,j \leq n} |\overline{c}_{ij}|) e_i^2$$
$$-(1 + \overline{k} - M)\overline{e}_i^2] dx. \tag{25}$$

Take $k > \alpha_2 + M + \beta n \max_{1 \leq i,j \leq n} |\overline{c}_{ij}|$ and $\overline{k} > M - 1$, then (25) can be estimated as:

$$\frac{\partial V(x,t)}{\partial t} \leq -\gamma \sum_{i=1}^{n} \int_{\Omega} \left[\frac{1}{2}(e_i^2 + \overline{e}_i^2) \right] dx, \tag{26}$$

where

$$\gamma = \min \left\{ 2(k - \alpha_2 - M - \beta n \max_{1 \leq i,j \leq n} |\overline{c}_{ij}|); 2(1 + \overline{k} - M) \right\}.$$

It can be found from (26) that $0 \leq V(x,t) \leq V(x,0)$, this together with (18) signifies $V(x,t)$ is bounded. Based on Lyapunov stability theory and LaSalle's invariance principle [4], we have:

$$\lim_{t \to +\infty} \sum_{i=1}^{n} \left(\|e_i\|_{L^2(\Omega)} + \|\overline{e}_i\|_{L^2(\Omega)} \right) = 0.$$

It follows from Definition 1 that the drive-response networks (5) and (6) achieve identical synchronization. Thus, the proof is complete. ■

III. Illustrative Numerical Examples

In this section, we present two examples of drive and response networks to illustrate the effectiveness of the method proposed in the previous section.

We have obtained numerical results that demonstrate identical synchronization between networks of reaction-diffusion systems of FHN and networks of reaction-diffusion systems of HR, despite having different network topologies. The systems were integrated using C++ and the results were visualized using Gnuplot.

Some parameters are fixed as [1], [2], [6], [7], [15], [16]:

$$f(u) = -u^3 + 3u, a = 1, b = 0.001, c = 0, \varepsilon = 0.1,$$
$$I_i = \overline{I}_i = 0, \; d_i = \overline{d}_i = 0.05, \; i = 1, 2, ..., n,$$
$$[0; T] \times \Omega = [0; 500] \times [0; 100] \times [0; 100],$$
$$\lambda = 10, \; V_{syn} = 2, \; \theta_{syn} = -0,25,$$
$$g(u) = -u^3 + \overline{a}u^2, \overline{a} = 3, \overline{b} = 5.$$

A. Example 1

In this example, we consider a ring network (drive network) with unidirectionally linear coupling, consisting of 3 nodes based on FHN:

$$\begin{cases} \varepsilon u_{1t} = f(u_1) - v_1 + I_1 + d_1\Delta u_1 - g_{syn}(u_1 - u_2) \\ v_{1t} = au_1 - bv_1 + c \\ \varepsilon u_{2t} = f(u_2) - v_2 + I_2 + d_2\Delta u_2 - g_{syn}(u_2 - u_3) \\ v_{2t} = au_2 - bv_2 + c \\ \varepsilon u_{3t} = f(u_3) - v_3 + I_3 + d_3\Delta u_3 - g_{syn}(u_3 - u_1) \\ v_{3t} = au_3 - bv_3 + c \end{cases} \tag{27}$$

and the response network consists of 3 nodes based on HR and is structured as a complete (full) network with linear coupling:

$$\begin{cases} \overline{u}_{1t} = g(\overline{u}_1) + \overline{v}_1 + \overline{I}_1 + \overline{d}_1\Delta\overline{u}_1 \\ \qquad -g_{syn}(\overline{u}_1 - \overline{u}_2) - g_{syn}(\overline{u}_1 - \overline{u}_3) + w_1 \\ \overline{v}_{1t} = 1 - \overline{b}\overline{u}_1^2 - \overline{v}_1 + \overline{w}_1 \\ \overline{u}_{2t} = g(\overline{u}_2) + \overline{v}_2 + \overline{I}_2 + \overline{d}_2\Delta\overline{u}_2 \\ \qquad -g_{syn}(\overline{u}_2 - \overline{u}_3) - g_{syn}(\overline{u}_2 - \overline{u}_1) + w_2 \\ \overline{v}_{2t} = 1 - \overline{b}\overline{u}_2^2 - \overline{v}_2 + \overline{w}_2 \\ \overline{u}_{3t} = g(\overline{u}_3) + \overline{v}_3 + \overline{I}_3 + \overline{d}_3\Delta\overline{u}_3 \\ \qquad -g_{syn}(\overline{u}_3 - \overline{u}_1) - g_{syn}(\overline{u}_3 - \overline{u}_2) + w_3 \\ \overline{v}_{3t} = 1 - \overline{b}\overline{u}_3^2 - \overline{v}_3 + \overline{w}_3 \end{cases} \tag{28}$$

with the adaptive controllers defined as:

$$\begin{cases} w_1 = u_{1t} - g(u_1) - v_1 - \overline{I}_1 - \overline{d}_1\Delta u_1 \\ \qquad +g_{syn}(u_1 - u_2) + g_{syn}(u_1 - u_3) - k_1(\bar{u}_1 - u_1) \\ w_2 = u_{2t} - g(u_2) - v_2 - \overline{I}_2 - \overline{d}_2\Delta u_2 \\ \qquad +g_{syn}(u_2 - u_1) + g_{syn}(u_2 - u_3) - k_2(\bar{u}_2 - u_2) \\ w_3 = u_{3t} - g(u_3) - v_3 - \overline{I}_3 - \overline{d}_3\Delta u_3 \\ \qquad +g_{syn}(u_3 - u_1) + g_{syn}(u_3 - u_2) - k_3(\bar{u}_3 - u_3) \\ \overline{w}_1 = v_{1t} - 1 + \overline{b}u_1^2 + v_1 - \overline{k}_1(\overline{v}_1 - v_1) \\ \overline{w}_2 = v_{2t} - 1 + \overline{b}u_2^2 + v_2 - \overline{k}_2(\overline{v}_2 - v_2) \\ \overline{w}_3 = v_{3t} - 1 + \overline{b}u_3^2 + v_3 - \overline{k}_3(\overline{v}_3 - v_3) \end{cases} \tag{29}$$

where

$$\begin{cases} k_{1t} = r_1(\overline{u}_1 - u_1)^2 \\ k_{2t} = r_2(\overline{u}_2 - u_2)^2 \\ k_{3t} = r_3(\overline{u}_3 - u_3)^2 \\ \overline{k}_{1t} = \overline{r}_1(\overline{v}_1 - v_1)^2 \\ \overline{k}_{2t} = \overline{r}_2(\overline{v}_2 - v_2)^2 \\ \overline{k}_{3t} = \overline{r}_3(\overline{v}_3 - v_3)^2 \end{cases} \tag{30}$$

Notice that the adaptive controllers (29) and the updated rules (30) are defined as (13), (14), and (15), respectively.

Fig. 2 below illustrates the synchronization errors of drive-response networks (27) and (28) without the adaptive controllers (29) and the updated rules (30). Specifically, Fig. 2(a), 2(b), 2(c) represent the synchronization errors of the coupled solutions, respectively:

$$(u_1(x_1,x_2,t), \overline{u}_1(x_1,x_2,t))\,,\ (u_2(x_1,x_2,t), \overline{u}_2(x_1,x_2,t))\,,$$
$$\text{and}\ \ (u_3(x_1,x_2,t), \overline{u}_3(x_1,x_2,t))$$

where $t \in [0;T]$ and for all $(x_1,x_2) \in \Omega$, with $g_{syn} = 0.1$. This figure illustrates that the synchronization errors do not approach zero, indicating that the drive-response networks are unable to achieve identical synchronization.

Fig. 3 below illustrates the synchronization errors of drive-response networks (27) and (28) with the adaptive controllers (29) and the updated rules (30). The simulations show that this adaptive scheme is effective and we can get:

$$\lim_{t\to+\infty} \sum_{i=1}^{3} \left(\|e_i\|_{L^2(\Omega)} + \|\overline{e}_i\|_{L^2(\Omega)} \right) = 0,$$

where $e_i = \overline{u}_i - u_i, \overline{e}_i = \overline{v}_i - v_i$, $i = 1,2,3$. Specifically, Fig. 3(a), 3(b), 3(c) represent the synchronization errors of the coupled solutions, respectively:

$$(u_1(x_1,x_2,t), \overline{u}_1(x_1,x_2,t))\,,\ (u_2(x_1,x_2,t), \overline{u}_2(x_1,x_2,t))\,,$$
$$\text{and}\ \ (u_3(x_1,x_2,t), \overline{u}_3(x_1,x_2,t))$$

where $t \in [0;T]$ and for all $(x_1,x_2) \in \Omega$, with $g_{syn} = 0.01, r_1 = 0.1, r_2 = 0.2, r_3 = 0.3$, $\overline{r}_1 = 0.1, \overline{r}_2 = 0.2, \overline{r}_3 = 0.3$. Here, we even take a smaller coupling strength than before. This figure shows that the synchronization errors reach zero, which means:

$$u_1(x_1,x_2,t) \approx \overline{u}_1(x_1,x_2,t),\ u_2(x_1,x_2,t) \approx \overline{u}_2(x_1,x_2,t)$$
$$\text{and}\ u_3(x_1,x_2,t) \approx \overline{u}_3(x_1,x_2,t),$$

for all $(x_1,x_2) \in \Omega$.

Fig. 4(a), 4(b), 4(c) represent the solutions $u_i(x_1,x_2,499), i = 1,2,3$, of the drive network (27) and Fig. 4(d), 4(e), 4(f) perform the solutions $\overline{u}_i(x_1,x_2,499)$, $i = 1,2,3$, of the response network (28). We can see that networks (27) and (28) have the same shape, i.e, the synchronization is performed.

B. Example 2

We are examining a 2-node drive network based on the FHN model. The network has a structure known as a complete (full) network with linear coupling.

$$\begin{cases} \varepsilon u_{1t} = f(u_1) - v_1 + I_1 + d_1\Delta u_1 - g_{syn}(u_1 - u_2) \\ v_{1t} = au_1 - bv_1 + c \\ \varepsilon u_{2t} = f(u_2) - v_2 + I_2 + d_2\Delta u_2 - g_{syn}(u_2 - u_1) \\ v_{2t} = au_2 - bv_2 + c \end{cases} \tag{31}$$

and the response network of 2 nodes based on HR that has the structure known as a chain network with nonlinear coupling is described by:

$$\begin{cases} \overline{u}_{1t} = g(\overline{u}_1) + \overline{v}_1 + \overline{I}_1 + \overline{d}_1\Delta\overline{u}_1 \\ \qquad -g_{syn}(\overline{u}_1 - V_{syn})\dfrac{1}{1+\exp(-\lambda(\overline{u}_2 - \theta_{syn}))} + w_1 \\ \overline{v}_{1t} = 1 - \overline{b}u_1^2 - v_1 + \overline{w}_1 \\ \overline{u}_{2t} = g(\overline{u}_2) + \overline{v}_2 + \overline{I}_2 + \overline{d}_2\Delta\overline{u}_2 + w_2 \\ \overline{v}_{2t} = 1 - \overline{b}u_2^2 - v_2 + \overline{w}_2 \end{cases} \tag{32}$$

with the adaptive controllers defined as:

$$\begin{cases} w_1 = u_{1t} - g(u_1) - v_1 - \overline{I}_1 - \overline{d}_1\Delta u_1 \\ \qquad +g_{syn}(u_1 - V_{syn})\dfrac{1}{1+\exp(-\lambda(u_2 - \theta_{syn}))} \\ \qquad -k_1(\bar{u}_1 - u_1) \\ w_2 = u_{2t} - g(u_2) - v_2 - \overline{I}_2 - \overline{d}_2\Delta u_2 - k_2(\bar{u}_2 - u_2) \\ \overline{w}_1 = v_{1t} - 1 + \overline{b}u_1^2 + v_1 - \overline{k}_1(\overline{v}_1 - v_1) \\ \overline{w}_2 = v_{2t} - 1 + \overline{b}u_2^2 + v_2 - \overline{k}_2(\overline{v}_2 - v_2) \end{cases} \tag{33}$$

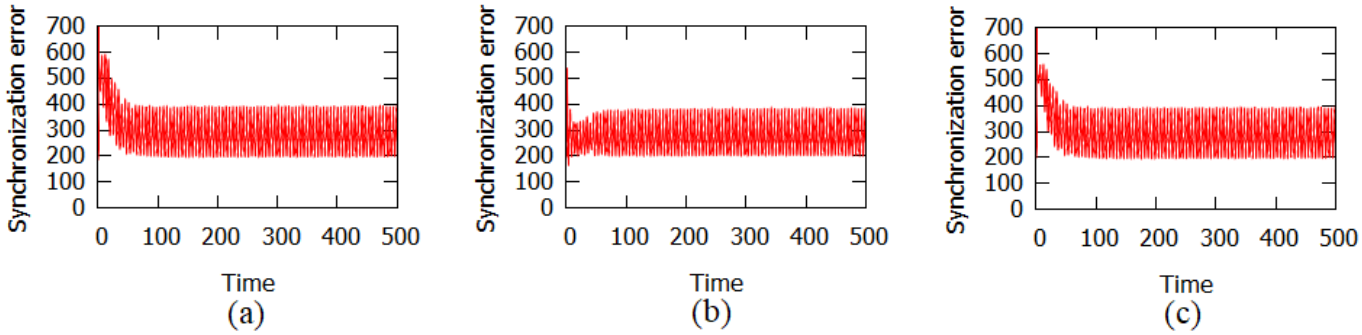

Fig. 2. Synchronization errors of the drive-response networks (27) and (28) without controllers (29). We can see that the synchronization errors do not reach zero which means there is not the synchronization.

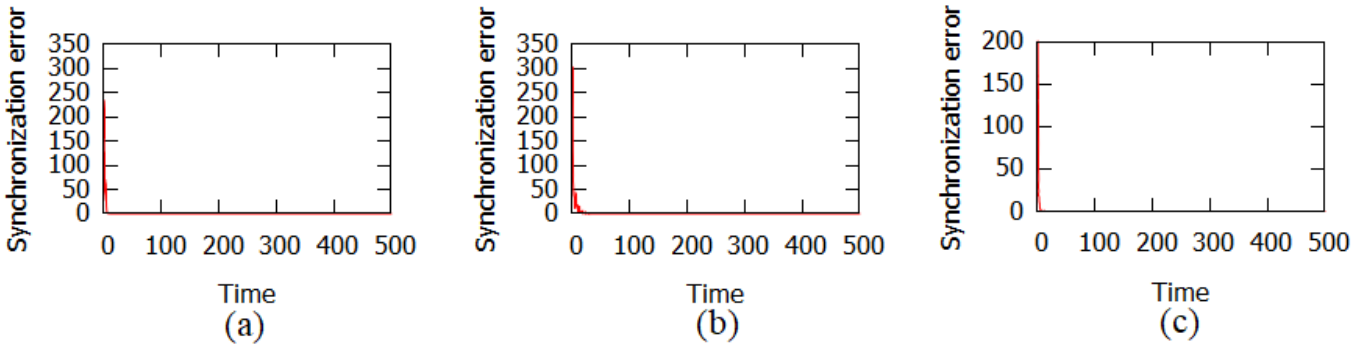

Fig. 3. Synchronization errors of the drive-response networks (27) and (28) with controllers (29). We can see that the synchronization errors asymptotically reaches zero which means the synchronization occurs.

where

$$\begin{cases} k_{1t} = r_1(\overline{u}_1 - u_1)^2 \\ k_{2t} = r_1(\overline{u}_2 - u_2)^2 \\ \overline{k}_{1t} = \overline{r}_1(\overline{v}_1 - v_1)^2 \\ \overline{k}_{2t} = \overline{r}_2(\overline{v}_2 - v_2)^2 \end{cases} \tag{34}$$

Notice that the adaptive controllers (33) and the updated rules (34) are defined as (13), (14), and (15), respectively.

Fig. 5 below illustrates the synchronization errors of drive-response networks (31) and (32) without the adaptive controllers (33) and the updated rules (34). Specifically, Fig. 5(a), 5(b) represent the synchronization errors of the coupled solutions, respectively:

$$(u_1(x_1, x_2, t), \overline{u}_1(x_1, x_2, t)),$$

and

$$(u_2(x_1, x_2, t), \overline{u}_2(x_1, x_2, t)),$$

where $t \in [0; T]$ and for all $(x_1, x_2) \in \Omega$, with $g_{syn} = 0.1$. This figure illustrates that the synchronization errors do not reach zero, indicating that the drive-response networks are unable to achieve identical synchronization.

Fig. 6 below illustrates the synchronization errors of drive-response networks (31) and (32) with the adaptive controllers (33) and the updated rules (34). The simulations show that this adaptive scheme is effective and we can get:

$$\lim_{t \to +\infty} \sum_{i=1}^{2} \left(\|e_i\|_{L^2(\Omega)} + \|\overline{e}_i\|_{L^2(\Omega)} \right) = 0,$$

where $e_i = \overline{u}_i - u_i, \overline{e}_i = \overline{v}_i - v_i$, $i = 1, 2$. Specifically, Fig. 6(a), 6(b) represent the synchronization errors of the coupled solutions, respectively:

$$(u_1(x_1, x_2, t), \overline{u}_1(x_1, x_2, t)),$$

and

$$(u_2(x_1, x_2, t), \overline{u}_2(x_1, x_2, t)),$$

where $t \in [0; T]$ and for all $(x_1, x_2) \in \Omega$, with $g_{syn} = 0.1, r_1 = 0.1, r_2 = 0.2$, $\overline{r}_1 = 0.1, \overline{r}_2 = 0.2$. This figure shows that the synchronization errors reach zero, which means:

$$u_1(x_1, x_2, t) \approx \overline{u}_1(x_1, x_2, t),$$

and

$$u_2(x_1, x_2, t) \approx \overline{u}_2(x_1, x_2, t),$$

for all $(x_1, x_2) \in \Omega$.

Fig. 7(a), 7(b) represent the solutions $u_i(x_1, x_2, 499), i = 1, 2$, of the drive network (31) and Fig. 7(c), 7(d) perform the solutions $\overline{u}_i(x_1, x_2, 499)$, $i = 1, 2$, of the response network (32). We can see that networks (31) and (32) have the same shape, i.e., the synchronization is performed.

Remark 7. Notice that the synchronization described above refers to the identical synchronization between two networks of cells. This means that the ith cell of the first network will exhibit the same pattern as the ith cell of the second network. In simpler terms, one network will mirror the behavior of the other. It is important to note that the behavior of cells within the same network can vary (refer to Fig. 4 and Fig. 7). However, if we aim for all cells in both networks to display the same pattern, we must increase the coupling strength so that it exceeds the necessary threshold value [6]. This way, all cells in both networks will exhibit the same pattern (as

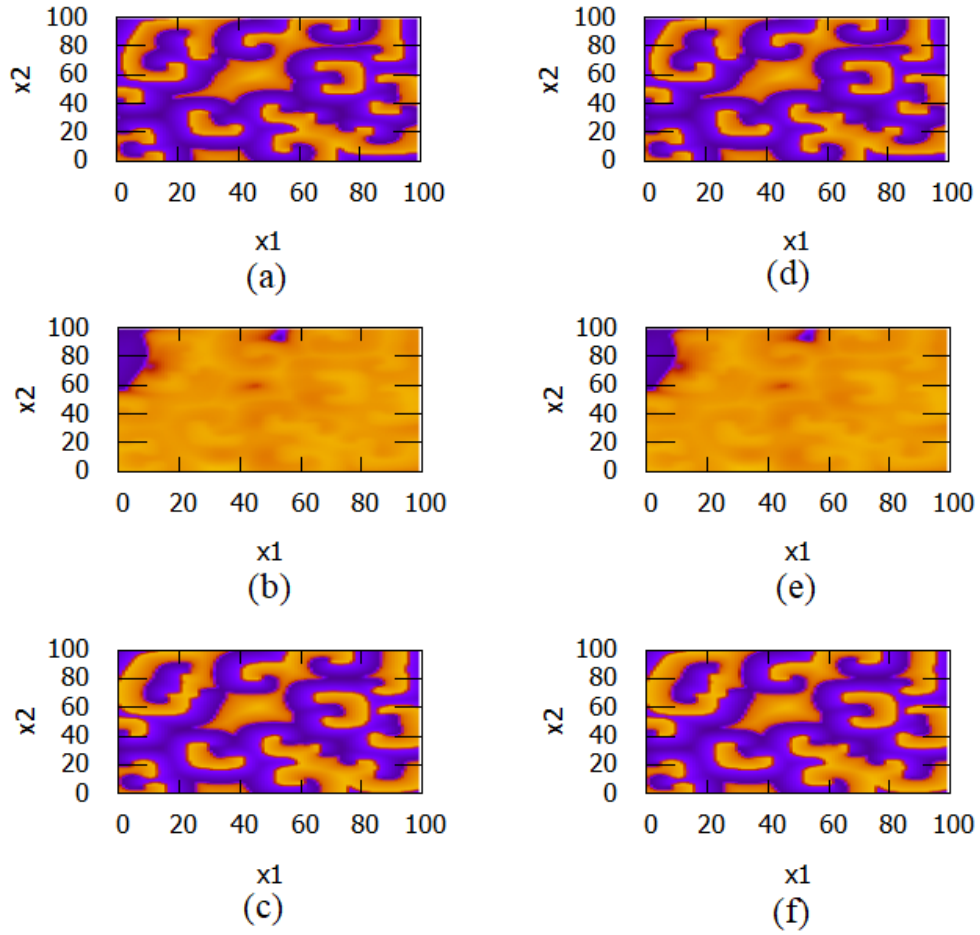

Fig. 4. Synchronization patterns of the drive-response networks (27) and (28) with controllers (29). Fig. 4(a), 4(b), 4(c) represent the solutions $u_i(x_1, x_2, 499), i = 1, 2, 3$, of the drive network (27), and Fig. 4(d), 4(e), 4(f), perform the solutions $\overline{u}_i(x_1, x_2, 499)$, $i = 1, 2, 3$, of the response network (28). We can observe that the patterns in the second column have the same shape as the patterns in the first column, respectively. In other words, the response network (27) synchronizes with the drive network (28).

depicted in Fig. 9). In Fig. 9, when we set $g_{syn} = 2$, this value is sufficiently large to ensure uniform behavior for all cells of networks (31) and (32).

Fig. 8(a), 8(b), 8(c), and 8(d) represent the synchronization errors of the coupled solutions, respectively:

$$(u_1(x_1, x_2, t), \overline{u}_1(x_1, x_2, t)), (u_2(x_1, x_2, t), \overline{u}_2(x_1, x_2, t)),$$

and

$$(u_1(x_1, x_2, t), u_2(x_1, x_2, t)), (\overline{u}_1(x_1, x_2, t), \overline{u}_2(x_1, x_2, t)),$$

where $t \in [0; T]$ and for all $(x_1, x_2) \in \Omega$, with $g_{syn} = 2, r_1 = 0.1, r_2 = 0.2$. This figure shows that the synchronization errors reach zero, which means:

$$u_1(x_1, x_2, t) \approx \overline{u}_1(x_1, x_2, t), u_2(x_1, x_2, t) \approx \overline{u}_2(x_1, x_2, t)$$

and

$$u_1(x_1, x_2, t) \approx u_2(x_1, x_2, t), \overline{u}_1(x_1, x_2, t) \approx \overline{u}_2(x_1, x_2, t)$$

for all $(x_1, x_2) \in \Omega$.

Fig. 9(a), 9(b) represent the solutions $u_i(x_1, x_2, 499), i = 1, 2$, of the drive network (31), and Fig. 9(c), 9(d) perform the solutions $\overline{u}_i(x_1, x_2, 499)$, $i = 1, 2$, of the response network (32). We can see that they have the same shape, i.e., the synchronization is performed for all cells of both networks.

IV. Conclusion

In this paper, we investigate the identical synchronization of drive-response neural networks consisting of different reaction-diffusion systems with arbitrary topological structures. Specifically, the drive network comprises n reaction-diffusion systems of FitzHugh-Nagumo type, while the response network contains n reaction-diffusion systems of Hindmarsh-Rose type. We develop nonlinear adaptive controllers and establish a suitable Lyapunov function to achieve the desired synchronization. The numerical results demonstrate the effectiveness of the proposed method. In this study, the use of complex synchronous controllers is necessary for attaining identical synchronization. Simplifying the controllers and exploring additional drive-response networks of n different reaction-diffusion systems will be key areas of investigation in future research.

References

[1] B. Ambrosio, M. A. Aziz-Alaoui, *Synchronization and control of coupled reaction-diffusion systems of the FitzHugh-Nagumo-type,* Computers and Mathematics with Applications, **64** (2012), 934-943.

[2] B. Ambrosio, M. A. Aziz-Alaoui, *Synchronization and control of a network of coupled reaction-diffusion systems of generalized FitzHugh-Nagumo type,* ESAIM: Proceedings, **39** (2013), 15-24.

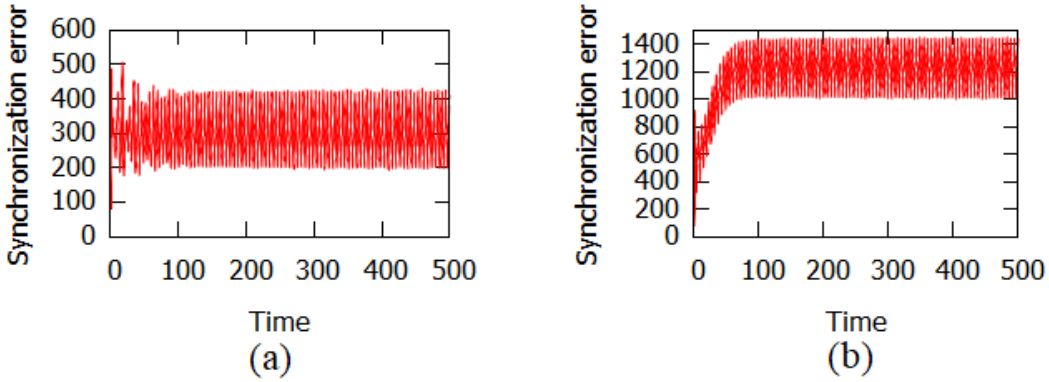

Fig. 5. Synchronization errors of the drive-response networks (31) and (32) without controllers (33). We can see that the synchronization errors do not reach zero which means there is not the synchronization.

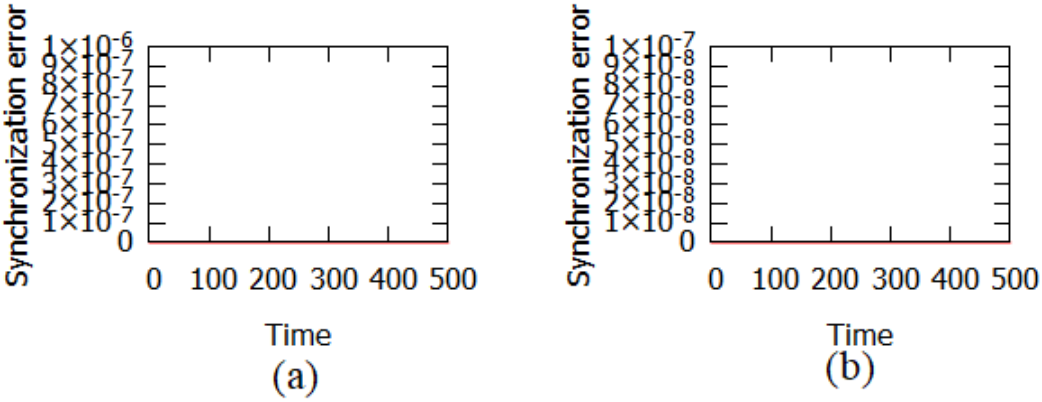

Fig. 6. Synchronization errors of the drive-response networks (31) and (32) with controllers (33). We can see that the synchronization errors asymptotically reaches zero which means the synchronization occurs.

[3] B. Ambrosio, M. A. Aziz-Alaoui, V. L. E. Phan, *Global attractor of complex networks of reaction-diffusion systems of Fitzhugh-Nagumo type,* American Institute of Mathematical Sciences, Discrete and Continuous Dynamical Systems series B, **23**(9) (2018), 3787-3797.

[4] D. Aeyels, *Asymptotic Stability of Nonautonomous Systems by Lyapunov's Direct Method,* Systems and Control Letters, **25** (1995) 273-280.

[5] M. A. Aziz-Alaoui, *Synchronization of Chaos,* Encyclopedia of Mathematical Physics, Elsevier, **5** (2006), 213-226.

[6] I. Belykh, E. De Lange, M. Hasler, *Synchronization of bursting neurons: What matters in the network topology,* Phys. Rev. Lett., (2005), 188101.

[7] N. Corson, *Dynamics of a neural model, synchronization and complexity,* PhD Thesis, University of Le Havre, France, (2009).

[8] G. B. Ermentrout, D. H. Terman, *Mathematical Foundations of Neurosciences,* Springer, (2009).

[9] J. L. Hindmarsh and R. M Rose, *A model of the nerve impulse using two first order differential equations,* Nature, **296** (1982), 162-164.

[10] A. L. Hodgkin, A. F. Huxley, *A quantitative description of membrane current and its application to conduction and excitation in nerve,* J. Physiol. **117** (1952), 500-544.

[11] E. M. Izhikevich, *Dynamical Systems in Neuroscience,* The MIT Press, (2007).

[12] D. W. Jordan, P. Smith, *Nonlinear Ordinary Differential Equations, An Introduction for Scientists and Engineers (4th Edition),* Oxford, (2007).

[13] J. P. Keener, J. Sneyd, *Mathematical Physiology,* Springer, (2009).

[14] J. D. Murray, *Mathematical Biology,* Springer, (2010).

[15] V. L. E. Phan, *Sufficient Condition for Synchronization in Complete Networks of Reaction-Diffusion Equations of Hindmarsh-Rose Type with Linear Coupling,* IAENG International Journal of Applied Mathematics, vol. **52**, no. 2 (2022), 315-319.

[16] V. L. E. Phan, *Sufficient Condition for Synchronization in Complete Networks of n Reaction-Diffusion Systems of Hindmarsh-Rose Type with Nonlinear Coupling,* Engineering Letters, vol. **31**(1) (2023), pp413-418.

[17] V. L. E. Phan, *Global Attractor of Networks of n Coupled Reaction-Diffusion Systems of Hindmarsh-Rose Type,* Engineering Letters, vol. **31**(3) (2023), pp1215-1220.

[18] V. L. E. Phan, *Identical synchronization in complete network of reaction-diffusion equations of Fitzhugh-Nagumo,* An Giang University International Journal of Sciences, **5** (2017), 51-58.

[19] V. L. E. Phan, *Synchronization in complete network of reaction-diffusion equations of Fitzhugh-Nagumo type with nonlinear coupling,* Can Tho University Journal of Science, Vol. **13**, No. 2 (2021), 43-51.

[20] V. L. E. Phan, *Synchronization in complete networks of ordinary differential equations of Fitzhugh-Nagumo type with nonlinear coupling,* Dong Thap University Journal of Science, Vol. **10**, No. 5 (2021), 3-9.

[21] A. Pikovsky, M. Rosenblum, J. Kurths, *Synchronization, A Universal Concept in Nonlinear Science,* Cambridge University Press, (2001).

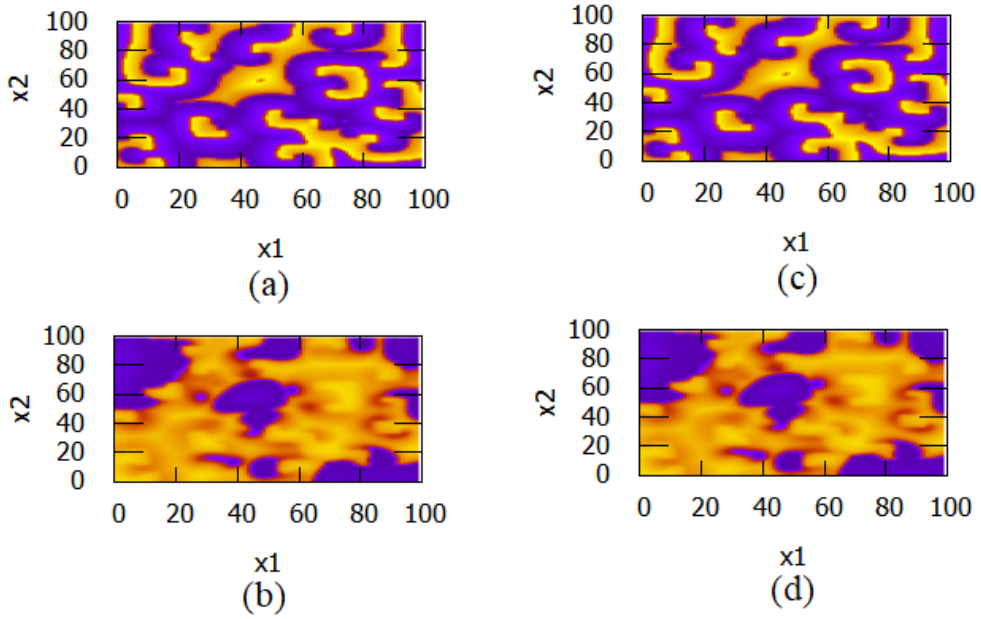

Fig. 7. Synchronization patterns of the drive-response networks (31) and (32) with controllers (33). Fig. 7(a), 7(b) represent the solutions $u_i(x_1, x_2, 499), i = 1, 2$, of the drive network (31), and Fig. 7(c), 7(d) perform the solutions $\overline{u}_i(x_1, x_2, 499)$, $i = 1, 2$, of the response network (32). We observe that the patterns in the second column mirror those in the first column. In other words, the response network in equation (31) synchronizes with the drive network in equation (32).

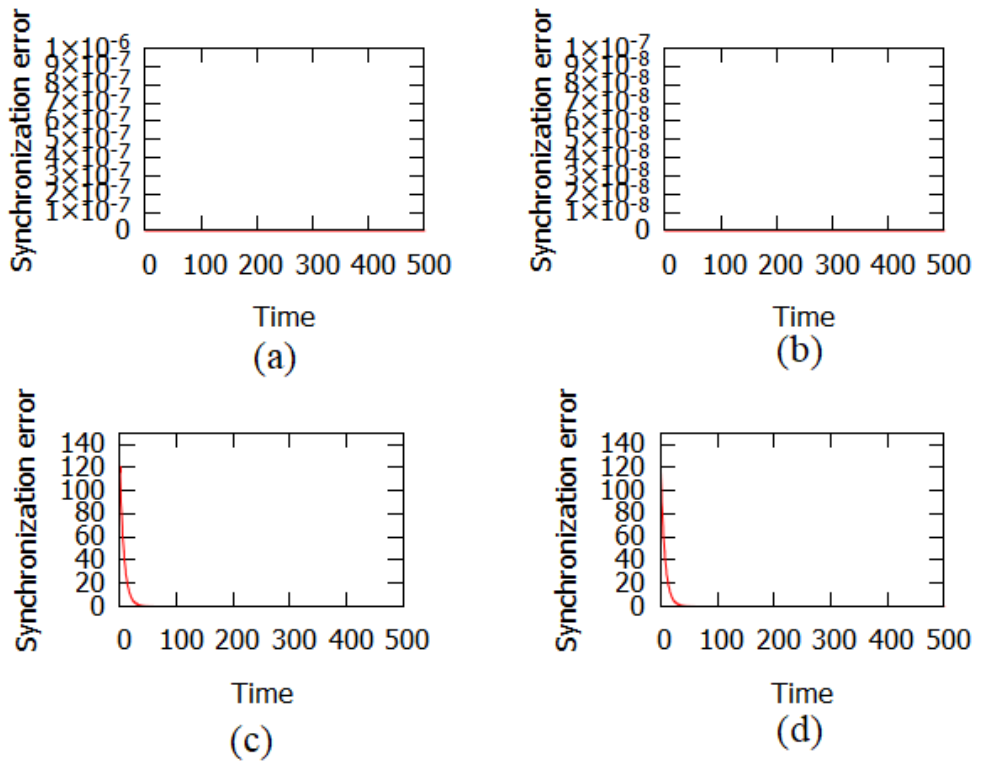

Fig. 8. Synchronization errors of the drive-response networks (31) and (32) with controllers (33) and big enough coupling strength. We can see that all synchronization errors asymptotically reaches zero which means the synchronization occurs for all nodes of both considering networks.

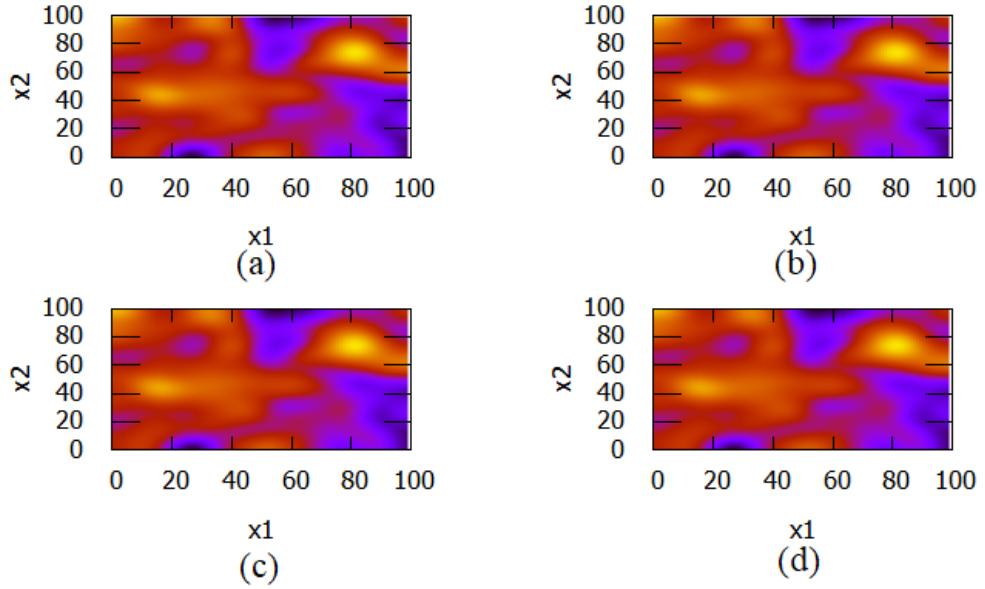

Fig. 9. Synchronization patterns of the drive-response networks (31) and (32) with controllers (33) and big enough coupling strength. Fig. 9(a), 9(b) represent the solutions $u_i(x_1, x_2, 499), i = 1, 2$, of the drive network (31), and Fig. 9(c), 9(d) perform the solutions $\overline{u}_i(x_1, x_2, 499)$, $i = 1, 2$, of the response network (32). We can see that all patterns have the same shape. In other words, the synchronization is performed for all cells of both networks.